Nanoparticle-Mediated Remote Control of Enzymatic Activity

Leslie D. Knecht,[†] Nur Ali,[‡] Yinan Wei,[§] J. Zach Hilt,[⊥,*] and Sylvia Daunert[∥,*]

[†]Department of Chemistry, University of Miami, Miami, Florida 33136, United States, [‡]Paul Laurence Dunbar High School, Lexington, Kentucky 40502, United States, [§]Department of Chemistry and [⊥]Department of Chemical and Materials Engineering, University of Kentucky, Lexington, Kentucky 40506, United States, and [∥]Department of Biochemistry and Molecular Biology, University of Miami, Miller School of Medicine, Miami, Florida 33136, United States

ABSTRACT

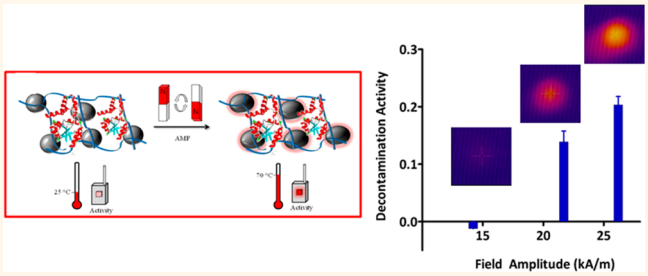

Nanomaterials have found numerous applications as tunable, remotely controlled platforms for drug delivery, hyperthermia cancer treatment, and various other biomedical applications. The basis for the interest lies in their unique properties achieved at the nanoscale that can be accessed *via* remote stimuli. These properties could then be exploited to simultaneously activate secondary systems that are not remotely actuatable. In this work, iron oxide nanoparticles are encapsulated in a bisacrylamide cross-linked polyacrylamide hydrogel network along with a model dehalogenase enzyme, L-2-HAD$_{ST}$. This thermophilic enzyme is activated at elevated temperatures and has been shown to have optimal activity at 70 °C. By exposing the Fe_3O_4 nanoparticles to a remote stimulus, an alternating magnetic field (AMF), enhanced system heating can be achieved, thus remotely activating the enzyme. The internal heating of the nanocomposite hydrogel network in the AMF results in a 2-fold increase in enzymatic activity as compared to the same hydrogel heated externally in a water bath, suggesting that the internal heating of the nanoparticles is more efficient than the diffusion-limited heating of the water bath. This system may prove useful for remote actuation of biomedical and environmentally relevant enzymes and find applications in a variety of fields.

KEYWORDS: dehalogenase · hydrogel nanocomposites · remote actuation · alternating magnetic field

Nanomaterials with unique energy-absorbing (*e.g.*, radio frequency, optical, *etc.*) and physical properties have built the foundation for a new field of remote controlled (RC) materials.[1−3] Due to such unique features, these materials have found many uses in medicine and biotechnology.[4−7] One example is the use of gold nanoshells for photothermal cancer therapy.[8] These materials absorb energy in the form of near-infrared light (NIR) and dissipate it as heat, which can be applied to induce photothermal ablation of cancer cells. Additionally, Wijaya *et al.* demonstrated that laser-induced melting of nanorods was shown to selectively release oligonucleotides from the nanorods, which may prove useful in drug delivery applications.[9] Carbon nanotubes (CNTs) have also been used for their unique heating abilities in the presence of NIR and other wavelengths of energy. Miyako *et al.* were able to control the activity of two thermophilic enzymes, Taq DNA polymerase and cyclomaltodextrin glucanotransferase, *via* heating CNTs with NIR laser irradiation.[10] This was one of the first demonstrations of remotely controlled enzymatic reactions using the heating properties of CNTs. Although these materials have been shown to be heated remotely, their uses *in vivo* are limited due to the minimal penetration depth of NIR light.[11] To overcome this limitation, nanoparticles have been explored as an alternative source for the production of localized heat when exposed to an alternating magnetic field (AMF).[12−14] Iron oxide nanoparticles are of particular interest because they not only function as heating sites and as vehicles for drug delivery, but they can also be visualized using conventional imaging techniques.[15−18] For instance, Thomas *et al.* developed a drug delivery system based on zinc-doped iron oxide nanocrystals encapsulated within mesoporous silica nanoparticles.[19] When heated in the presence of an AMF, temperature-responsive valves opened to release the encapsulated drug. Importantly, it was demonstrated that no compound was released in the absence of the field. Recently, Stanley *et al.* demonstrated that, by coating iron oxide nanoparticles with antibodies, they could be targeted to a temperature-sensitive Ca^{2+} ion channel.[20] When the nanoparticles are heated with an AMF, the channels open, allowing for an influx of Ca^{2+} ions. In turn, a bioengineered Ca^{2+}-driven

* Address correspondence to sdaunert@med.miami.edu; hilt@uky.edu.

Received for review July 23, 2012 and accepted September 18, 2012.

Published online September 18, 2012
10.1021/nn303308v

promoter is activated, thus intitiating the transcription of insulin. This is one of the first examples of using the heating properties of iron oxide nanoparticles to remotely control gene expression.

Nanocomposites containing magnetic nanoparticles have also been used to enhance or control the properties of stimuli-responsive hydrogels.[21−24] There are numerous classes of stimuli-responsive hydrogels that have been developed and are able to, depending on their composition, respond reversibly to external stimuli such as temperature, pH, electric potential, and analyte concentration.[25−27] By combining the remote heating capabilities of the nanoparticles with the stimuli-responsive properties of hydrogels, multifunctional materials can be designed for targeted applications such as drug delivery, hyperthermia cancer treatment, and as stimuli-responsive microfluidic valves.[13,28−30] Zadrazil *et al.* encapsulated iron oxide nanoparticles in a thermo-responsive polymer, poly(*N*-isopropylacrylamide) (PNIPAM) to form a temperature-responsive hydrogel sponge that could release an oil, kerosene, in the presence of an alternating magnetic field.[31] It was demonstrated that, by combining the hydrophilic responsive polymer with the iron oxide nanoparticles, a drug delivery system for hydrophobic compounds could be developed with on-demand release by exposure to an AMF.

Herein, we demonstrate that by combining enzyme-modified responsive hydrogels with Fe_3O_4 nanomaterials, RC nanocomposites can be developed that could find applications not only in the remote decontamination of environmental samples but also as "on/off" switches for heating and activating proteins in other biomedical, industrial, and pharmaceutical applications. Specifically, the incorporated Fe_3O_4 nanoparticles controllably heat the hydrogel matrix in the presence of an AMF, thus allowing for the remote control of the temperature within the system.[13] By exploiting this selective heating capability, enhancement of catalytic activity was achieved by turning on the coencapsulated thermophilic enzyme. The reactivity of the biomolecules is enhanced at higher temperatures (Figure 1a), where combining the divergent materials results in a remotely controlled system. Specifically, we demonstrated the ability to remotely activate a model enzyme, L-2-HAD_{ST}, a thermophilic dehalogenase isolated and characterized from the thermophile archaea *Sulfolobus tokodaii*. This enzyme catalyzes the stereospecific dehalogenation of L-2-haloalkanoates to D-2-hydroxyalkanoates (Figure 1b). By encapsulating the enzyme into the hydrogel, it allows for the use of the biocatalyst through many enzymatic cycles with different substrates without the need for complicated separation and/or regeneration steps.

RESULTS AND DISCUSSION

L-2-HAD_{ST} catalyzes the dehalogenation of organic compounds, such as the model substrate

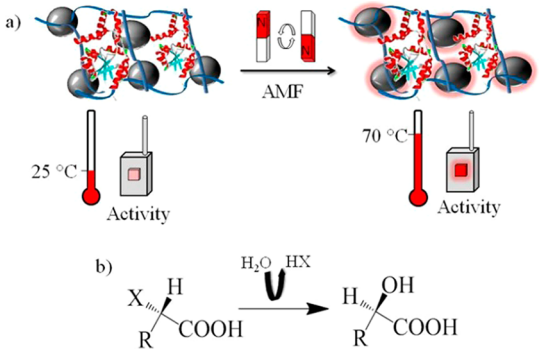

Figure 1. (a) L-2-HAD_{ST} immobilized in a hydrogel network containing Fe_3O_4 nanoparticles. At room temperature, the enzyme activity is minimal. In the presence of the AMF, the nanoparticles heat, thus heating the environment around the L-2-HAD_{ST} and increasing the activity of the enzyme. (b) L-2-HAD_{ST} functions by replacing the halogen (X) on an L-2-haloalkanoate with a hydroxyl group. The result is the formation of an D-2-hydroxyalkanoate.

S-2-chloropropionic acid (CPA). The reaction results in the stereospecific dehalogenation of CPA and formation free chloride, which can be measured by a chloride ion-selective electrode (ISE). L-2-HAD_{ST} has optimal activity at pH 9.5 and 70 °C and maintains its activity when immobilized on a solid matrix.[32] The demonstration of the long-term activity of the enzyme in solution, as well as its ability to work under extreme conditions and retain activity upon immobilization, allowed us to formulate the hypothesis that L-2-HAD_{ST} can maintain its enzymatic activity after chemical conjugation to acrylic acid monomers and polymerization into a hydrogel network. Purification of the enzyme used for all of the studies was performed using a previously established protocol.[32] After purification, L-2-HAD_{ST} was incorporated into a hydrogel network by chemical conjugation to acrylic acid functional groups *via* the lysines on the protein. An acrylamide hydrogel containing the L-2-HAD_{ST} was then polymerized with 1.5 wt % bisacrylamide cross-linking in the presence of 10% (w/v) Fe_3O_4 nanoparticles. Previous modeling studies indicated that such a nanoparticle concentration would be needed to reach and maintain the desired temperatures.[33] Additionally, a control hydrogel was polymerized by replacing the enzyme solution with the same volume of 20 mM glycine buffer, pH 9.5. The hydrogel was used as a mechanism by which encapsulation of both the enzyme and the nanoparticles was possible, thereby allowing for remote heating of the system in the presence of an AMF. This is envisioned to allow for activation of the system for bioremediation capabilities with facile recollection of the materials when the process is finished. Although this technique was implemented to immobilize the enzyme in the hydrogel, other strategies may be employed to directly immobilize enzymes to the nanoparticles.[34] The immobilization can lead to enhanced stability of the enzyme, as previously demonstrated.[35]

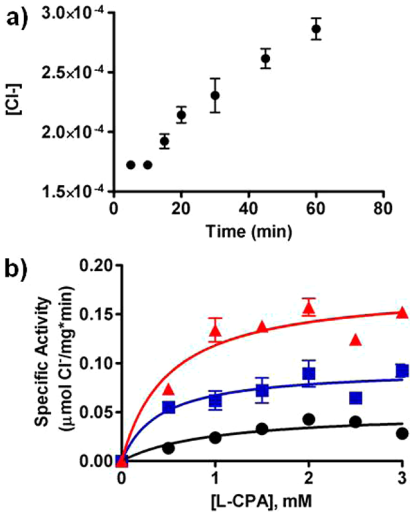

Figure 2. (a) Protein was encapsulated in the hydrogel, and a time study was performed by allowing the nanocomposite hydrogel pieces to incubate with 0.5 mM CPA for various periods of time. Data are blank subtracted and shown as averages ± one standard deviation (n = 3). The time point chosen for subsequent experiments was 30 min. (b) To test the activity of the immobilized protein, the hydrogel-encapsulated L-2-HAD$_{ST}$ was incubated for 30 min at 21 °C (circles), 50 °C (squares), and 70 °C (triangles) with various concentrations of CPA. Data are blank subtracted and shown as averages ± one standard deviation (n = 3).

With the enzyme incorporated into the hydrogel network, a time study was conducted to determine the optimal incubation time for the substrate. The hydrogel-encapsulated enzyme was incubated with 0.5 mM CPA for various periods of time ranging from 10 min to 1 h at 70 °C. The incubation time used for subsequent studies was determined to be 30 min (Figure 2a). Although the time study showed a constant increase in activity over the hour incubation, the 30 min time point is long enough to detect activity significantly above the blank, yet short enough to optimize assay time. After determining the time of incubation for the hydrogel-encapsulated enzyme with the substrate, it was important to demonstrate the activity trend when exposed to varying temperatures. To demonstrate temperature effects on activity, we evaluated the enzyme turnover at three different temperatures (~21, 50, and 70 °C). The highest temperature chosen was 70 °C, the optimal temperature for enzyme activity. Higher temperatures were not used because the aim of the study was to evaluate if the enzyme could be remotely heated using an AMF, not to determine stability of the hydrogel-encapsulated enzyme. First, the activity of the hydrogel-encapsulated enzyme at room temperature (RT, ~21 °C) was evaluated. The hydrogels were placed in a 20 mM glycine buffer, pH 9.5, containing various substrate concentrations (Figure 2b). After incubating for 30 min, the hydrogels were removed and the chloride concentration was measured. For each substrate concentration, triplicate measurements were performed using hydrogels containing the enzyme and control hydrogels prepared in the absence of the enzyme. The latter was used to determine the contribution of substrate autohydrolysis during the incubation period, which was taken into account by subtracting the chloride concentration in the controls from the total chloride concentration in the test samples. The protein in the hydrogel was found to have a k_{cat} of (4.02 ± 0.18) × 10^{-5} s^{-1} and a K_m of 1.03 ± 0.27 mM. Furthermore, the enzymatic efficiency at room temperature was found to be (0.39 ± 0.10) × 10^{-4} mM^{-1} s^{-1}.

Next, the activity of the hydrogel-encapsulated enzyme was evaluated at 50 °C, which is still lower than the optimum temperature for reactivity (70 °C). The experiments were performed as described above by incubating for 30 min at 50 °C in a water bath. After the incubation period, the hydrogels were removed and the samples allowed to cool to room temperature before measuring the chloride concentration. The enzyme was found to have a k_{cat} of (17.9 ± 2.6) × 10^{-5} s^{-1} and a K_m of 0.41 ± 0.01 mM. The enzymatic efficiency was (4.39 ± 0.65) × 10^{-4} mM^{-1} s^{-1}, representing a >7-fold increase in functionality as compared to the system at room temperature, which was expected as L-2-HAD$_{ST}$ is a thermophilic enzyme with optimal reactivity observed at higher temperatures. Additionally, the K_m also decreased at 50 °C compared to the hydrogel at room temperature. This demonstrates that the enzyme is still able to more favorably bind the substrate for enzymatic activity at the higher temperature when encapsulated in the hydrogel.

Finally, the experiments were repeated as above by incubating the hydrogels for 30 min in a water bath at 70 °C, the optimum temperature for enzymatic activity. The k_{cat} was determined to be (27.6 ± 0.6) × 10^{-5} s^{-1}, the K_m was 0.52 ± 0.15 mM, while the enzymatic efficiency was (5.33 ± 1.54) × 10^{-4} mM^{-1} s^{-1}. The efficiency increased by almost 1.5 times when the hydrogel-encapsulated enzyme was heated at 70 °C as compared to 50 °C and by ~15-fold as compared to the enzyme at room temperature. This remarkable increase in activity as a function of temperature is based upon the thermophilic nature of the system. To that end, higher temperatures are required for maximal activity. The K_m value did not vary significantly for the enzyme at 70 °C as compared to 50 °C. Previously published studies also suggest that the K_m values at these temperatures are comparable.[32,36] Unfortunately, global heating of the system, which includes the hydrogel and surrounding environment, is highly energy inefficient and can result in unwanted side effects. This is especially true when applying the materials for selective functionality in a complex matrix.

Studies were also carried out to characterize the free enzyme in order to compare its activity to that of the enzyme immobilized in the hydrogel network. A time study was performed using 2.0 mM of CPA (Figure 3a),

which demonstrated an optimal incubation time at 70 °C of 10 min. Next, L-2-HAD$_{ST}$ was incubated with various concentrations of substrate in 20 mM glycine buffer, pH 9.5, for 10 min, and its activity was measured by determining the concentration of chloride with an ISE. Characterization of the Michaelis–Menten kinetics (Figure 3b) found a k_{cat} of (213.4 ± 8.7) × 10^{-5} s^{-1}, K_m of 1.25 ± 0.16 mM, and an enzymatic efficiency (k_{cat}/K_m) of (17.02 ± 2.28) × 10^{-4} mM^{-1} s^{-1}. The activity of the free enzyme in the water bath at 70 °C was compared to the hydrogel-encapsulated enzyme at varying temperatures, as summarized in Table 1. From this study, it was determined that the enzymatic efficiency of the immobilized enzyme was about 30% of the efficiency of the free enzyme at the same temperature; however, activity was maintained even after protein modification and hydrogel encapsulation. A decrease in enzymatic efficiency was seen previously when the enzyme was immobilized on a sepharose resin.[36] The decreased enzymatic efficiency observed in our study is likely due to the immobilization of the enzyme in the hydrogel network and the diffusion limitation of the substrate into the hydrogel.[37,38] By conjugating the enzyme to the hydrogel through nonspecific lysines, some protein may become denaturated, or the enzymatic pocket may become inaccessible to the substrate as a result of immobilization. Even so, the enzymatic efficiency increased with increasing the temperature from room temperature to the optimum temperature for activity (70 °C) within the hydrogel. This suggests that although there may be enzyme molecules where the binding pocket is inaccessible to the substrate, there is a significant fraction of immobilized enzyme that maintains function.

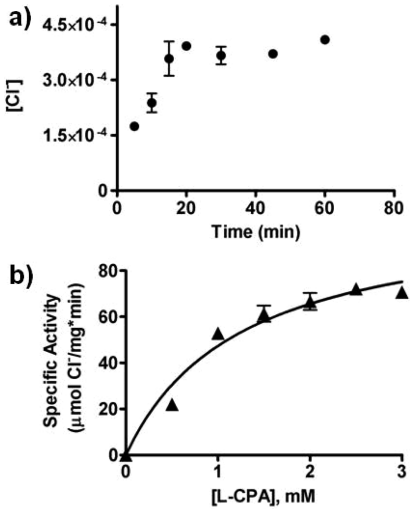

Figure 3. (a) Time study of the free L-2-HAD$_{ST}$. The protein was incubated at 70 °C with 2 mM CPA for various periods of time. Data are blank subtracted and shown as averages ± one standard deviation (n = 3). The optimal incubation time chosen was 10 min. (b) To test the activity of the free protein, 0.003 mg of L-2-HAD$_{ST}$ was incubated at 70 °C in the presence of various concentrations of CPA for 10 min. Data are blank subtracted and shown as averages ± one standard deviation (n = 3).

Once the above parameters were established, we hypothesized that the hydrogel with encapsulated Fe_3O_4 nanoparticles could be heated remotely *via* an AMF, thus increasing the activity of the incorporated enzyme. Successful remote heating would allow for use of the materials in self-contained remote sites, making them ideal for environmental field applications. Initially, studies were performed with the hydrogel-encapsulated enzyme containing Fe_3O_4 nanoparticles to ensure that it could be remotely heated to 70 °C, which is required for optimum L-HAD$_{ST}$ activity. The hydrogels were exposed to a magnetic field amplitude of 19.9 kA/m for 15 min on an induction power supply equipped with a solenoid (1.5 cm diameter, 5 turns). Using this approach, the temperature of the hydrogel was measured every 30 s with an infrared thermal imaging camera. Approximately 2.5 min into the exposure, the hydrogel heated to 70 °C and maintained that temperature for at least 15 min (Figure 4a). The images taken using the IR camera demonstrate that when the hydrogel was not in the presence of the AMF (time = 0), there is no heating. After exposure to the AMF after 60 s, the hydrogel begins to heat up and continues to do so until about 150 s. At this time, the hydrogel is at the maximum temperature for that field amplitude, and it maintains that temperature until the field is removed (Figure 4b). Although this study was important to demonstrate that the temperature could be controlled in a narrow range by heating with the AMF, the temperatures were measured with an IR camera and not in solution. Due to the need for the hydrogel–air interface, the parameters used in this study may not directly correlate to the system when immersed in buffer. Therefore, further optimization for the hydrogel heating had to be conducted for the hydrogel in solution. This was assessed by using 0.5 mM substrate and measuring L-2-HAD$_{ST}$ activity after a 10 min exposure time to various magnetic field amplitudes (14.2, 21.7, 26.2, and 30.6 kA/m).

TABLE 1. Summary of Kinetic Data for L-2-HAD$_{ST}$ under Various Conditions[a]

	FP, 70 °C[b]	HE, 21 °C	HE, 50 °C[b]	HE, 70 °C[b]	HE, AMF
k_{cat} (×10^{-5} s^{-1})	213.4 ± 8.7	4.02 ± 0.18	17.9 ± 2.6	27.6 ± 0.6	31.3 ± 8.1
K_m (mM)	1.25 ± 0.16	1.03 ± 0.27	0.41 ± 0.01	0.52 ± 0.15	0.30 ± 0.07
k_{cat}/K_m (×10^{-4} mM^{-1} s^{-1})	17.02 ± 2.28	0.39 ± 0.10	4.39 ± 0.65	5.33 ± 1.54	10.11 ± 3.52

[a] Data are shown as averages ± one standard deviation (n = 3). FP, free protein; HE, hydrogel-encapsulated protein. [b] Incubation in a water bath at the specified temperature.

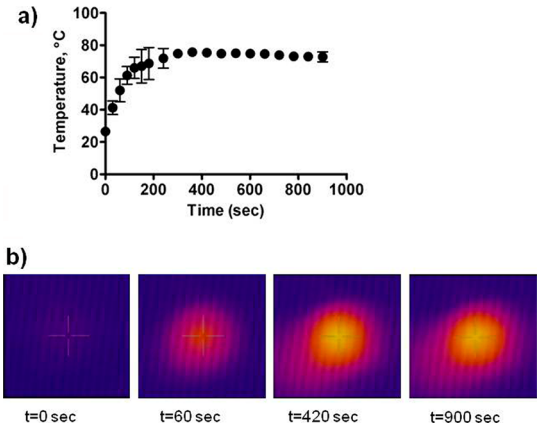

Figure 4. Demonstration of heating capabilities of the nanocomposite hydrogels when exposed to the AMF. The hydrogels were exposed to a magnetic field amplitude of 19.9 kA/m for 15 min on an induction power supply equipped with a solenoid (1.5 cm diameter, 5 turns). (a) The temperature was plotted at each time point, and (b) A picture was taken with an IR camera every 30 sec. The IR images of four time points (0 sec, 60 sec, 420, and 900 sec) are shown.

As a control, the hydrogels were incubated with 0.5 mM substrate for 10 min at room temperature in the absence of the AMF. The control chloride concentration was then subtracted from the values found in the samples exposed to the field to ensure that the enzyme activity was due to the field and not to other environmental factors. As expected, as the field amplitude increased, the activity of the enzyme increased; however, as the amplitude passed 26.2 kA/m, the activity decreased (Figure 5a). This is consistent with previous data where the activity of free L-HAD$_{ST}$ decreased after the temperature increased over 70 °C, possibly due to protein denaturation.[32] Although this study does not allow for direct correlation of field amplitude to temperature, it demonstrated that the activity of the enzyme followed a similar trend in the presence of the AMF as it did when heated in the water bath. Therefore, it was determined that the optimum activity was obtained at a field amplitude of 26.2 kA/m, which was used for all subsequent activity experiments. Characterization of the remotely heated hydrogels was performed by determining enzymatic activity after a 10 min incubation time at 26.2 kA/m in the presence of various substrate concentrations (Figure 5b). From this study, the enzyme was determined to have a k_{cat} of (31.3 ± 8.1) × 10^{-5} s^{-1} and a K_m of 0.30 ± 0.07 mM. The catalytic efficiency of L-2-HAD$_{ST}$ was found to be (10.11 ± 3.52) × 10^{-4} mM^{-1} s^{-1} (Table 1). The k_{cat} increased when the hydrogel was heated with an AMF, and the K_m decreased. This suggests that the affinity of the substrate to the enzyme increased when heated with the AMF, which indicates that the remote heating is a more efficient heating method for optimal activity as compared to external approaches. Furthermore, the increase in k_{cat} demonstrates that the product turnover is higher when heated in the AMF as compared to the

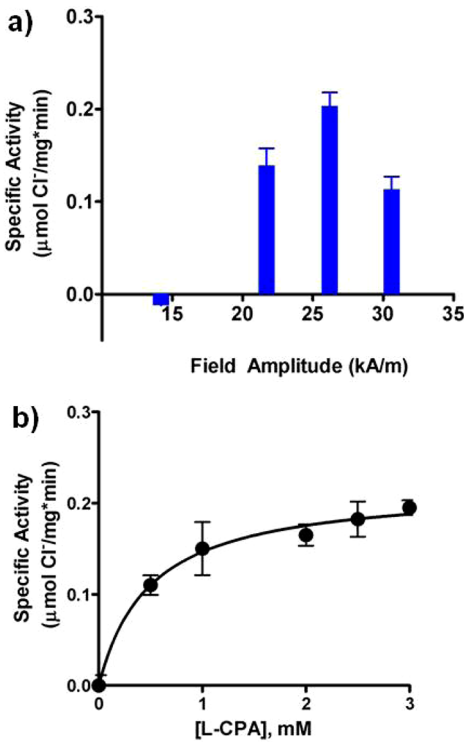

Figure 5. (a) To find an optimal power setting on the alternating magnetic field, the hydrogels were incubated in the specified field strength for 10 min in the presence of 0.5 mM CPA. The optimum field amplitude was determined to be 26.2 kA/m. (b) Hydrogels were then placed at this field strength in the presence of various substrate concentrations. After 10 min incubation, the chloride concentrations were measured to calculate the specific activity of the enzyme. Data are blank subtracted and shown as averages ± one standard deviation (n = 3).

water bath. This is interesting because the time of exposure, and thus the heating, in the AMF (10 min) is three times less than in the water bath (30 min), which indicates that the enzyme reaches and maintains the optimal temperature more rapidly in the AMF. Interestingly, compared to the free protein, the k_{cat} of the immobilized enzyme does decrease. Such results were previously observed when the enzyme was immobilized *via* the lysine residues on sepharose beads.[36] The k_{cat} of the free enzyme is roughly 10 times greater than the encapsulated materials, which, as discussed previously, likely arises from the diffusion limitation of the substrate through the porous hydrogel and the modification of the enzyme for hydrogel encapsulation. It is important to note, however, that the purpose of this study was not to compare the activity of the free and hydrogel-encapsulated protein but to evaluate the efficiency of remotely controlling the heating of the enzyme in a system that is easily recoverable. Therefore, the more significant value in this work is the comparison of the k_{cat} of the hydrogel-encapsulated enzyme heated in the water bath *versus* heated in the AMF.

To study the long-term stability of the enzyme-encapsulated hydrogel, the same nanocomposite systems

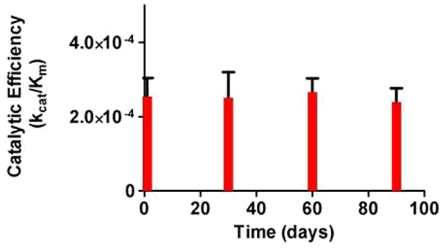

Figure 6. Demonstration of long-term stability of hydrogel-encapsulated enzyme over a three month period. Each month, the hydrogels were incubated with varying substrate concentrations and heated *via* a water bath at 70 °C. Data are shown as averages ± one standard deviation (n = 3).

were used over a three month period. The specific activity was calculated and plotted every month for three months. Enzymatic activity was maintained even after storage at 4 °C in glycine buffer for the three month period (Figure 6). As evident, no decrease in activity was observed over this time period, indicating potential long-term stability.

On the basis of our results, numerous enhancements over conventional enzymatic applications can be achieved using the nanocomposite system. First, the data show that the catalytic efficiency increased 2-fold when the hydrogels were heated *via* the AMF instead of the water bath at 70 °C. Furthermore, the sample incubation time for the AMF system required heating for only 10 min, as compared to 30 min required by the water bath. The system not only has efficient localized heating but also requires less time to achieve higher catalytic output as compared to the hydrogel in the water bath. This is because the AMF exposure generates highly localized heating at the reaction location in the system. Due to the encapsulated Fe_3O_4 nanoparticles, the system reaches higher internal temperatures more rapidly than when using traditional heating methods. Unfortunately, the internal temperature of the hydrogel could not be determined, but this could be predicted through modeling/simulations[33] or determined after the development of an appropriate measurement technique. Second, upon the basis of the design of the composite system, recyclability of the functional materials can be readily achieved. By having magnetic materials encapsulated in the hydrogel, magnetic separation can be applied to extract the functional materials from complex mixtures. This is important for the long-term recyclability, while minimizing the need to produce excessive amounts of enzyme. To that end, multiple sets of the composite material were functional for at least a three month period.

CONCLUSIONS

In conclusion, the formation of a novel composite system for remote controlled enzymatic activity has been demonstrated. This system consists of a hydrogel, a thermophilic enzyme, and magnetic nanoparticles for remote heating in the presence of an AMF. The activity of the system was enhanced *via* AMF-based heating as compared to conventional heating methods due to the composite nature of the materials. Such materials can be readily dispersed in environmental systems for facile, remote contaminant degradation that is difficult to achieve using current technologies. It is envisioned that our approach can be applied to the creation of other materials that incorporate biological or synthetic elements that can be activated *via* an on/off switch and used in a variety of industrial, environmental, and medical applications.

METHODS

Chemicals and Apparatus. Sodium hydroxide, sodium chloride, ammonium persulfate (APS), sodium phosphate dibasic, sodium phosphate monobasic, acrylamide, and bisacrylamide were purchased from Sigma (St. Louis, MO). S-2-chloropropionic acid, acrylic acid, 1-ethyl-3-[3-dimethylaminopropyl]carbodiimide hydrochloride (EDC), *N*-hydroxysulfosuccinimide (Sulfo-NHS), tetramethylethylenediamine (TEMED), and glycine were obtained from Fisher Scientific (Pittsburgh, PA). All chemicals were reagent grade or better. All solutions were prepared using reverse osmosis water (Milli-Q Water Purification System, Millipore, Bedford, MA). Nanoparticles were purchased from Nanostructured & Amorphous Materials Inc. (Houston, TX). The 15 mL centrifuge tubes were purchased from Sarstedt (Newton, NC). Chloride concentrations were determined using a chloride ion-selective electrode (VWR, West Chester, PA). Alternating magnetic field studies were performed on an induction power supply (MMF-3-135/400-2, Taylor Winfield, Brookfield, OH) equipped with a solenoid (1.5 cm diameter, 5 turns). All results were analyzed using GraphPad Prism version 5.0 (GraphPad Software, Inc., La Jolla, CA).

Enzymatic Activity Determination of Free L-2-HAD$_{ST}$ Using the Chloride ISE. A stock solution of CPA (10 mM) substrate was prepared in glycine buffer (20 mM, pH 9.5). After addition of the substrate to the buffer, the pH was readjusted with NaOH to 9.5. From this stock solution, dilutions of CPA (0, 0.5, 1.0, 1.5, 2.0, 2.5, and 3.0 mM) were prepared in glycine buffer (20 mM, pH 9.5). Triplicate aliquots (2 mL) were obtained from each CPA solution. Then, L-2-HAD$_{ST}$ (0.003 mg) was added to each sample and incubated for 10 min at 70 °C. Blank samples were prepared by adding an equivalent volume of glycine buffer to the protein without substrate. Upon cooling, a commercial chloride ISE was used to determine chloride concentration.

Hydrogel Fabrication. The first step of the covalent immobilization of the L-2-HAD$_{ST}$ into a hydrogel network involved the chemical conjugation of the lysine residues of the enzyme to the carboxylic groups of acrylic acid monomers using well-established carbodiimide-mediated coupling reaction protocols. First, acrylic acid (170 μL of a 1 × 10^{-3} M stock solution) was added to a reaction mixture of EDC (0.115 mg) and sulfo-NHS (0.575 mg) and left to react at room temperature for 15 min. To this mixture was added enzyme (2.0 mg) at RT for 2 h and left to react, without stirring, at 4 °C overnight. The conjugated protein was then centrifuged in an Amicon centrifuge filter with a 3000 MW cutoff to remove any unreacted acrylic acid.

Before polymerization of the hydrogels, the hydrogel cast was weighed and the mass recorded. For hydrogel fabrication, acrylamide (300 mg) and bisacrylamide (576 μL) were added to 2-(*N*-morpholino)ethanesulfonic acid (MES) buffer (2.35 mL, pH 5.5). Next, Fe_3O_4 (10% w/v) nanoparticles were added to

the precursor solution, which was then sonicated for 20 min to disperse the Fe_3O_4 nanoparticles. After dispersion, either (2 mL, 1 mg/mL) of the L-2-HAD_{ST}-acrylamide functionalized enzyme or buffer (control hydrogels) was added to the solution. Next, APS (60 μL) and TEMED (25 μL) were incorporated into the solution, and the hydrogels were allowed to polymerize for 1 h at 4 °C. After the solution was warmed to room temperature, the hydrogel and cast were again weighed. The mass of the cast was subtracted from the mass of the hydrogel plus cast to get an accurate mass of the hydrogel. The polymerized matrix was then removed from the cast and washed overnight in 20 mM glycine buffer, pH 9.5, to remove any of the unreacted monomer from the hydrogel. The hydrogels were then cut into 4 mm diameter round pieces. Eight of these pieces were weighed and their masses averaged. This average was expressed as a percent of the total hydrogel mass. To estimate the average mass of protein in each hydrogel piece, the percentage of mass found for an individual piece was multiplied by the total protein concentration incorporated into the hydrogel matrix.

Determination of Hydrogel-Encapsulated L-2-HAD_{ST} Activity in a Water Bath. A stock solution CPA (10 mM) substrate was prepared in glycine buffer (20 mM, pH 9.5). After addition of the substrate to the buffer, the pH was readjusted with NaOH to 9.5. From this stock solution, dilutions of CPA (0, 0.5, 1.0, 1.5, 2.0, 2.5, and 3.0 mM) were prepared in glycine buffer (20 mM, pH 9.5). Triplicate aliquots (2 mL) were obtained from each CPA solution. Hydrogel pieces were added to the solutions that either contained the immobilized L-2-HAD_{ST} or no protein (control hydrogels). Each sample was incubated for 30 min at 21 °C (room temperature), 50 °C (water bath), or 70 °C (water bath). They hydrogel pieces were immediately removed. Upon cooling to room temperature, a commercial chloride ISE was used to determine chloride concentration.

Long-Term Stability of Hydrogel-Encapsulated L-2-HAD_{ST} in a Water Bath. The activity of the enzyme was determined as described above. Specific activity was evaluated at 70 °C each month for three months from the same set of hydrogels.

Alternating Magnetic Field Studies. The hydrogels with the encapsulated enzyme and control hydrogels were incubated at various field amplitudes for 10 min in the presence of CPA (0.5 mM). Simultaneously, hydrogels with the encapsulated enzyme and control hydrogels were also incubated for 10 min in the presence of CPA (0.5 mM) at room temperature. Next, the hydrogel was removed from solution, and the chloride concentration was measured. All measurements were blank subtracted to account for the chloride formation at room temperature. After determining the field amplitude for optimum enzymatic activity, an assay was performed to evaluate the enzymatic efficiency. Stock solutions of the substrate were prepared as described above. The hydrogels were exposed to a field amplitude of 26.2 kA/m for 10 min in the presence of various amounts of substrate as described previously, then the hydrogel was removed and the chloride concentration determined *via* the chloride ISE.

Time Study of Free L-2-HAD_{ST}. A time study was performed to find an optimal incubation time for L-2-HAD_{ST} activity. The substrate concentration was kept constant at 2.0 mM S-2-chloropropionic acid in 20 mM glycine buffer, pH 9.5. Each sample in triplicate was incubated for the desired time (5, 10, 15, 30, 45, and 60 min) in a water bath at 70 °C. After incubation, the tubes were cooled to room temperature and a commercial chloride ISE was used to determine chloride concentration.

Time Study of Hydrogel-Encapsulated L-2-HAD_{ST}. The hydrogels were incubated in a 20 mM glycine buffer, pH 9.5, with 0.5 mM substrate for different time intervals (5, 10, 15, 20, 30, 45, and 60 min) in a water bath at 70 °C. After incubation, the hydrogels were removed and the samples allowed to cool to room temperature. The chloride concentration was then determined *via* a commercial chloride ISE.

Heating Profile of Hydrogel. The wet hydrogel was wrapped in saran wrap and placed on the top of the coil of the AMF apparatus. The field strength was set at 19.9 kA/m, and the temperature of the hydrogel was visualized using an AGEMA Thermovision 470 IR camera (FLIR, Boston, MA).

Conflict of Interest: The authors declare no competing financial interest.

Acknowledgment. The authors would like to thank the National Science Foundation Grant ECC-08017788 and the National Institute of Environmental Health Sciences Grant P42ES07380 for funding this work. S.D. thanks the University of Kentucky for a Gill Eminent Professorship and the Miller School of Medicine of the University of Miami for the Lucille P. Markey Chair in Biochemistry and Molecular Biology. L.D.K. would like to thank the National Science Foundation Integrative Graduate Education Research Traineeship (Grant DGE-0653710).

REFERENCES AND NOTES

1. Pan, Y.; Du, X.; Zhao, F.; Xu, B. Magnetic Nanoparticles for the Manipulation of Proteins and Cells. *Chem. Soc. Rev.* **2012**, *41*, 2912–2942.
2. Huschka, R.; Zuloaga, J.; Knight, M. W.; Brown, L. V.; Nordlander, P.; Halas, N. J. Light-Induced Release of DNA from Gold Nanoparticles: Nanoshells and Nanorods. *J. Am. Chem. Soc.* **2011**, *133*, 12247–12255.
3. Alkilany, A. M.; Thompson, L. B.; Boulos, S. P.; Sisco, P. N.; Murphy, C. J. Gold Nanorods: Their Potential for Photothermal Therapeutics and Drug Delivery, Tempered by the Complexity of Their Biological Interactions. *Adv. Drug Delivery Rev.* **2012**, *64*, 190–199.
4. Schroeder, A.; Goldberg, M.; Kastrup, C.; Levins, C. G.; Langer, R. S.; Anderson, D. G. Remotely Activated Protein-Producing Nanoparticles. *Nano Lett.* **2012**, *12*, 2685–2689.
5. Fabbro, A.; Villari, A.; Laishram, J.; Scaini, D.; Toma, F. M.; Turco, A.; Prato, M.; Ballerini, L. Spinal Cord Explants Use Carbon Nanotube Interfaces To Enhance Neurite Outgrowth and To Fortify Synaptic Inputs. *ACS Nano* **2012**, *6*, 2041–2055.
6. Park, J. H.; von Maltzahn, G.; Xu, M. J.; Fogal, V.; Kotamraju, V. R.; Ruoslahti, E.; Bhatia, S. N.; Sailor, M. J. Cooperative Nanomaterial System To Sensitize, Target, and Treat Tumors. *Proc. Natl. Acad. Sci. U.S.A.* **2010**, *107*, 981–986.
7. Dreaden, E. C.; Alkilany, A. M.; Huang, X.; Murphy, C. J.; El-Sayed, M. A. The Golden Age: Gold Nanoparticles for Biomedicine. *Chem. Soc. Rev.* **2012**, *41*, 2740–2779.
8. Morton, J. G.; Day, E. S.; Halas, N. J.; West, J. L. Nanoshells for Photothermal Cancer Therapy. *Methods Mol. Biol.* **2010**, *624*, 101–117.
9. Wijaya, A.; Schaffer, S. B.; Pallares, I. G.; Hamad-Schifferli, K. Selective Release of Multiple DNA Oligonucleotides from Gold Nanorods. *ACS Nano* **2009**, *3*, 80–86.
10. Miyako, E.; Nagata, H.; Hirano, K.; Hirotsu, T. Laser-Triggered Carbon Nanotube Microdevice for Remote Control of Biocatalytic Reactions. *Lab Chip* **2009**, *9*, 788–794.
11. Ntziachristos, V.; Ripoll, J.; Weissleder, R. Would Near-Infrared Fluorescence Signals Propagate through Large Human Organs for Clinical Studies? *Opt. Lett.* **2002**, *27*, 1652.
12. Frimpong, R. A.; Fraser, S.; Hilt, J. Z. Synthesis and Temperature Response Analysis of Magnetic-Hydrogel Nanocomposites. *J. Biomed. Mater. Res., Part A* **2007**, *80*, 1–6.
13. Satarkar, N. S.; Biswal, D.; Hilt, J. Z. Hydrogel Nanocomposites: A Review of Applications as Remote Controlled Biomaterials. *Soft Matter* **2010**, *6*, 2364–2371.
14. Hamad-Schifferli, K.; Schwartz, J. J.; Santos, A. T.; Zhang, S.; Jacobson, J. M. Remote Electronic Control of DNA Hybridization through Inductive Coupling to an Attached Metal Nanocrystal Antenna. *Nature* **2002**, *415*, 152–155.
15. Tietze, R.; Lyer, S.; Durr, S.; Alexiou, C. Nanoparticles for Cancer Therapy Using Magnetic Forces. *Nanomedicine* **2012**, *7*, 447–457.
16. Al Faraj, A.; Gazeau, F.; Wilhelm, C.; Devue, C.; Guerin, C. L.; Pechoux, C.; Paradis, V.; Clement, O.; Boulanger, C. M.; Rautou, P. E. Endothelial Cell-Derived Microparticles Loaded with Iron Oxide Nanoparticles: Feasibility of MR Imaging Monitoring in Mice. *Radiology* **2012**, *263*, 169–178.

17. Burtea, C.; Laurent, S.; Mahieu, I.; Larbanoix, L.; Roch, A.; Port, M.; Rousseaux, O.; Ballet, S.; Murariu, O.; Toubeau, G.; *et al. In Vitro* Biomedical Applications of Functionalized Iron Oxide Nanoparticles, Including Those Not Related to Magnetic Properties. *Contrast Media Mol. Imaging* **2011**, *6*, 236–250.
18. Tartaj, P.; Morales, M. D.; Veintemillas-Verdaguer, S.; Gonzalez-Carreno, T.; Serna, C. J. The Preparation of Magnetic Nanoparticles for Applications in Biomedicine. *J. Phys. D: Appl. Phys.* **2003**, *36*, R182–R197.
19. Thomas, C. R.; Ferris, D. P.; Lee, J. H.; Choi, E.; Cho, M. H.; Kim, E. S.; Stoddart, J. F.; Shin, J. S.; Cheon, J.; Zink, J. I. Noninvasive Remote-Controlled Release of Drug Molecules *in Vitro* Using Magnetic Actuation of Mechanized Nanoparticles. *J. Am. Chem. Soc.* **2010**, *132*, 10623–10625.
20. Stanley, S. A.; Gagner, J. E.; Damanpour, S.; Yoshida, M.; Dordick, J. S.; Friedman, J. M. Radio-Wave Heating of Iron Oxide Nanoparticles Can Regulate Plasma Glucose in Mice. *Science* **2012**, *336*, 604–608.
21. Haraguchi, K.; Takehisa, T. Nanocomposite Hydrogels: A Unique Organic–Inorganic Network Structure with Extraordinary Mechanical, Optical, and Swelling/Deswelling Properties. *Adv. Mater.* **2002**, *14*, 1120–1124.
22. Pardo-Yissar, V.; Gabai, R.; Shipway, A. N.; Bourenko, T.; Willner, I. Gold Nanoparticle/Hydrogel Composites with Solvent-Switchable Electronic Properties. *Adv. Mater.* **2001**, *13*, 1320–1323.
23. Satarkar, N. S.; Johnson, D.; Marrs, B.; Andrews, R.; Poh, C.; Gharaibeh, B.; Saito, K.; Anderson, K. W.; Hilt, J. Z. Hydrogel-MWCNT Nanocomposites: Synthesis, Characterization, and Heating with Radiofrequency Fields. *J. Appl. Polym. Sci.* **2010**, *117*, 1813–1819.
24. Zhao, X.; Ding, X.; Deng, Z.; Zheng, Z.; Peng, Y.; Tian, C.; Long, X. A Kind of Smart Gold Nanoparticle–Hydrogel Composite with Tunable Thermo-Switchable Electrical Properties. *New J. Chem.* **2006**, *30*, 915–920.
25. Hilt, J. Z.; Byrne, M. E.; Peppas, N. A. Microfabrication of Intelligent Biomimetic Networks for Recognition of D-Glucose. *Chem. Mater.* **2006**, *18*, 5869–5875.
26. Liedl, T.; Dietz, H.; Yurke, B.; Simmel, F. Controlled Trapping and Release of Quantum Dots in a DNA-Switchable Hydrogel. *Small* **2007**, *3*, 1688–1693.
27. Wei, B.; Cheng, I.; Luo, K. Q.; Mi, Y. Capture and Release of Protein by a Reversible DNA-Induced Sol–Gel Transition System. *Angew. Chem., Int. Ed.* **2008**, *47*, 331–333.
28. Hao, R.; Xing, R.; Xu, Z.; Hou, Y.; Gao, S.; Sun, S. Synthesis, Functionalization, and Biomedical Applications of Multifunctional Magnetic Nanoparticles. *Adv. Mater.* **2010**, *22*, 2729–2742.
29. Satarkar, N. S.; Hilt, J. Z. Magnetic Hydrogel Nanocomposites for Remote Controlled Pulsatile Drug Release. *J. Controlled Release* **2008**, *130*, 246–251.
30. Satarkar, N. S.; Zhang, W.; Eitel, R. E.; Hilt, J. Z. Magnetic Hydrogel Nanocomposites as Remote Controlled Microfluidic Valves. *Lab Chip* **2009**, *9*, 1773–1779.
31. Zadrazil, A.; Tokarova, V.; Stepanek, F. Remotely Triggered Release from Composite Hydrogel Sponges. *Soft Matter* **2012**, *8*, 1811–1816.
32. Bachas-Daunert, P. G.; Law, S. A.; Wei, Y. Charicterization of a Recombinant Thermostable Dehalogenase Isolated from the Hot Spring Thermophile *Sulfolobus tokodaii*. *Appl. Biochem. Biotechnol.* **2009**, *159*, 382–393.
33. Satarkar, N. S.; Meenach, S. A.; Anderson, K. W.; Hilt, J. Z. Remote Actuation of Hydrogel Nanocomposites: Heating Analysis, Modeling, and Simulations. *AIChE J.* **2011**, *57*, 852–860.
34. Cude, M. P.; Gwenin, C. D. Development of Gold Coated Superparamagnetic Iron Oxide Nanoparticles for Nitroreductase Delivery. *ECS Trans.* **2011**, *33*, 79–89.
35. Ren, Y. H.; Rivera, J. G.; He, L. H.; Kulkarni, H.; Lee, D. K.; Messersmith, P. B. Facile, High Efficiency Immobilization of Lipase Enzyme on Magnetic Iron Oxide Nanoparticles *via* a Biomimetic Coating. *BMC Biotechnol.* **2011**, *11*, 63.
36. Bachas-Daunert, P. G.; Sellers, Z. P.; Wei, Y. Detection of Halogenated Organic Compounds Using Immobilized Thermophilic Dehalogenase. *Anal. Bioanal. Chem.* **2009**, *395*, 1173–1178.
37. Cardenas-Fernandez, M.; Lopez, C.; Alvaro, G.; Lopez-Santin, J. L-Phenylalanine Synthesis Catalyzed by Immobilized Aspartate Aminotransferase. *Biochem. Eng. J.* **2012**, *63*, 15–21.
38. Grosova, Z.; Rosenberg, M.; Rebros, M.; Sipocz, M.; Sedlackova, B. Entrapment of β-Galactosidase in Polyvinylalcohol Hydrogel. *Biotechnol. Lett.* **2008**, *30*, 763–767.